Video Article

A Novel Stretching Platform for Applications in Cell and Tissue Mechanobiology

Dominique Tremblay[1], Charles M. Cuerrier[1,2], Lukasz Andrzejewski[1], Edward R. O'Brien[3], Andrew E. Pelling[1,4,5]

[1]Centre for Interdisciplinary NanoPhysics, Department of Physics, University of Ottawa

[2]University of Ottawa Heart Institue, University of Ottawa

[3]Libin Cardiovascular Institute of Alberta, University of Calgary

[4]Department of Biology, University of Ottawa

[5]Institute for Science, Society and Policy, University of Ottawa

Correspondence to: Andrew E. Pelling at a@pellinglab.net

URL: https://www.jove.com/video/51454
DOI: doi:10.3791/51454

Keywords: Bioengineering, Issue 88, cell stretching, tissue mechanics, nuclear mechanics, uniaxial, biaxial, anisotropic, mechanobiology

Date Published: 6/3/2014

Citation: Tremblay, D., Cuerrier, C.M., Andrzejewski, L., O'Brien, E.R., Pelling, A.E. A Novel Stretching Platform for Applications in Cell and Tissue Mechanobiology. *J. Vis. Exp.* (88), e51454, doi:10.3791/51454 (2014).

Abstract

Tools that allow the application of mechanical forces to cells and tissues or that can quantify the mechanical properties of biological tissues have contributed dramatically to the understanding of basic mechanobiology. These techniques have been extensively used to demonstrate how the onset and progression of various diseases are heavily influenced by mechanical cues. This article presents a multi-functional biaxial stretching (BAXS) platform that can either mechanically stimulate single cells or quantify the mechanical stiffness of tissues. The BAXS platform consists of four voice coil motors that can be controlled independently. Single cells can be cultured on a flexible substrate that can be attached to the motors allowing one to expose the cells to complex, dynamic, and spatially varying strain fields. Conversely, by incorporating a force load cell, one can also quantify the mechanical properties of primary tissues as they are exposed to deformation cycles. In both cases, a proper set of clamps must be designed and mounted to the BAXS platform motors in order to firmly hold the flexible substrate or the tissue of interest. The BAXS platform can be mounted on an inverted microscope to perform simultaneous transmitted light and/or fluorescence imaging to examine the structural or biochemical response of the sample during stretching experiments. This article provides experimental details of the design and usage of the BAXS platform and presents results for single cell and whole tissue studies. The BAXS platform was used to measure the deformation of nuclei in single mouse myoblast cells in response to substrate strain and to measure the stiffness of isolated mouse aortas. The BAXS platform is a versatile tool that can be combined with various optical microscopies in order to provide novel mechanobiological insights at the sub-cellular, cellular and whole tissue levels.

Video Link

The video component of this article can be found at https://www.jove.com/video/51454/

Introduction

The mechanical microenvironment plays an important role in many cell functions such as proliferation, migration, and differentiation, which have a profound impact in the development and homeostasis of tissues and also in diseases[1-6]. Over the years, a multitude of experimental tools have been used to mechanically stimulate cells or tissues and measure mechanical properties of biological tissues with the goal of increasing our understanding of basic mechanobiology and studying the onset and progression of diseases[6-17]. However, one must often rely on several different experimental devices in order to achieve the goals of a particular study. This article presents a single, multi-functional, biaxial stretching (BAXS) platform that allows for studies that investigate the role that mechanical properties and mechanical forces play in biology at the sub-cellular to whole tissue length scales. The BAXS platform not only allows for the quantification of the mechanical properties of isolated tissues, but also facilitates the ability to apply simple, complex, and dynamic strain fields to living cells in order to understand their responses to stretching that occurs *in vivo*. The BAXS platform also maintains the capacity to perform live-cell microscopy during mechanical testing and perturbations on cells and tissues.

The BAXS platform is a custom-built apparatus that can be used to investigate the effect of substrate deformation at the cellular level and perform tensile tests on biological tissues (**Figure 1A**). An aluminum heater was fabricated to accommodate a standard 10-cm Petri dish and maintain any physiological solutions at 37 °C using a temperature controller and kapton heaters (**Figure 1B**). This BAXS platform can be integrated onto an inverted phase contrast and/or fluorescence microscope and allows for simultaneous imaging (**Figure 1C**). In brief, the BAXS platform consists of four linear voice coil motors of which the moving parts are mounted on miniature linear motion ball bearing slides oriented along two perpendicular axes (**Figure 1D**). A linear positioning stage is mounted to each of the four motors to allow vertical movement of the clamping system that will be used (**Figure 1E**). The position of each motor is monitored by an optical encoder with a resolution of 500 nm (**Figure 1F**). All four motors are independently controlled with a motion controller employing optical encoder feedback to execute motion

commands (**Figure 1G**). A LabVIEW interface provides full control over the displacement magnitude, speed, and acceleration of each motor in order to generate completely customizable, static and dynamic, deformation of the cells or tissue samples.

The technique used to induce a deformation in cells is achieved by simply allowing cells to firmly adhere to a flexible and transparent substrate and then stretching this substrate using the four motors of the BAXS platform. The BAXS platform allows mounting of any custom-designed set of clamps to attach the substrate on the voice coil motors. For this purpose, we designed a set of clamps to which a flexible and transparent substrate, made of polydimethylsiloxane (PDMS), can be attached (**Figures 2A-C** and **Figure 3**). As the clamps will be exposed to physiological solutions, all parts were machined from stainless steel to allow for sterilization. These clamps have been carefully designed to bring the substrate as close as possible to the microscope objective to enhance image quality while minimizing the stress on the substrate during stretching (**Figure 2D**).

The same BAXS platform can also be used to quantify the stiffness of small tissue samples, using an appropriate set of clamps with adapted supports for the tissue samples and a load cell to monitor forces. Several approaches can be taken to mount a tissue to the BAXS platform motors; in this case the stainless steel insect minutiens pins can hook through the opening of vascular tissues in order to perform tensile tests (**Figures 4A-B**). Alternatively, for thick tissues without a natural opening, tissue edges can either be held in position with the clamps attached to the voice coil motors or glued to small glass slides with biological glue and attached to the motors with the clamps. In order to perform tensile tests a miniature load cell is required and can be easily incorporated onto the BAXS platform motors and used to measure the force acting on the tissue during a stretching cycle (**Figure 4C**). As the BAXS platform is composed of four motors, the introduction of a second load cell allows one to perform tensile testing along two orthogonal directions. This ability allows one to quantify the mechanical stiffness of a single tissue along two perpendicular directions during the same experiment.

Importantly, in all configurations, the cells or tissue samples of interest are always maintained in a temperature-controlled bath that is accessible to the user. This ability allows for the introduction of pharmacological agents during sample stretching in order to examine the temporal response of the sample. Additionally, as the optical axis of the inverted microscope remains unobstructed, all forms of microscopy are still available to the user. Finally, as all four motors of the BAXS platform are independent it is possible to apply highly configurable strain fields to the sample of interest. *In vivo* cells and tissues are exposed to complex and anisotropic stretching that can be more appropriately mimicked in this platform as opposed to traditional uniaxial stretching platform[7,13,15,18,19]. Moreover, the physical characteristics of the strain field can be changed on the fly during an experiment. These abilities allow the user to examine the cellular and tissue level response to a wide number of highly complex, anisotropic, temporally, and spatially varying strain fields. This article describes the advantages and limitations of the BAXS platform as well as its design, operating principles, and the experimental details for single cell and whole tissue experiments.

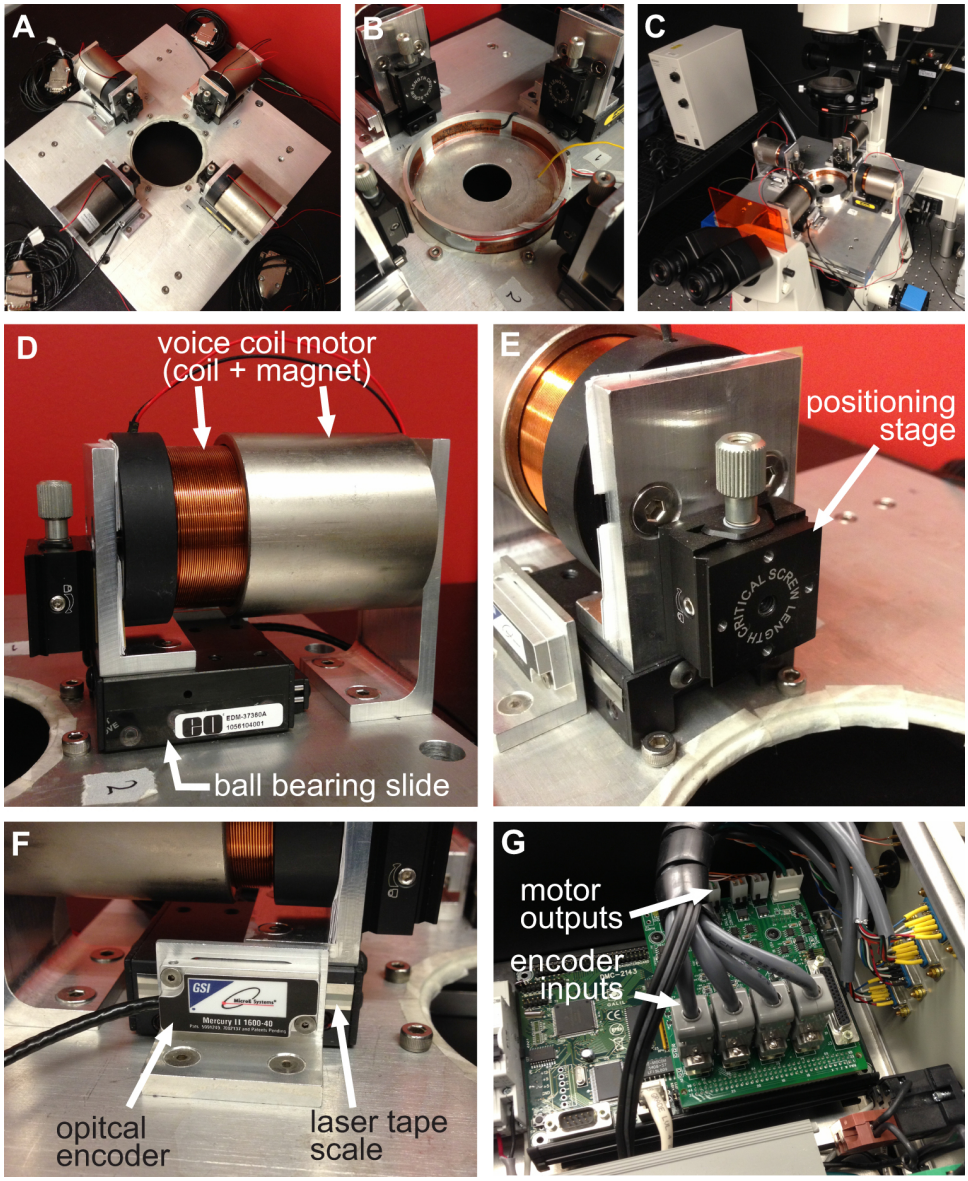

Figure 1. Overview of the BAXS platform. A) Top view of the BAXS platform showing the four voice coil motors. **B**) Detailed picture of the Petri dish heater used to maintain cells and tissues at 37 °C. **C**) The platform can be mounted on an inverted microscope to perform live-cell imaging during stretching experiments. **D**) Detailed picture of the voice coil motor; the moving part of the platform. **E**) Detailed picture of the linear positioning stage allowing vertical displacement of the clamping systems. **F**) Detailed picture of the optical encoder that provides real-time position of the motor to the motion controller. **G**) Detailed picture of the motion controller showing the four optical encoder inputs and power outputs to the four voice coil motors.

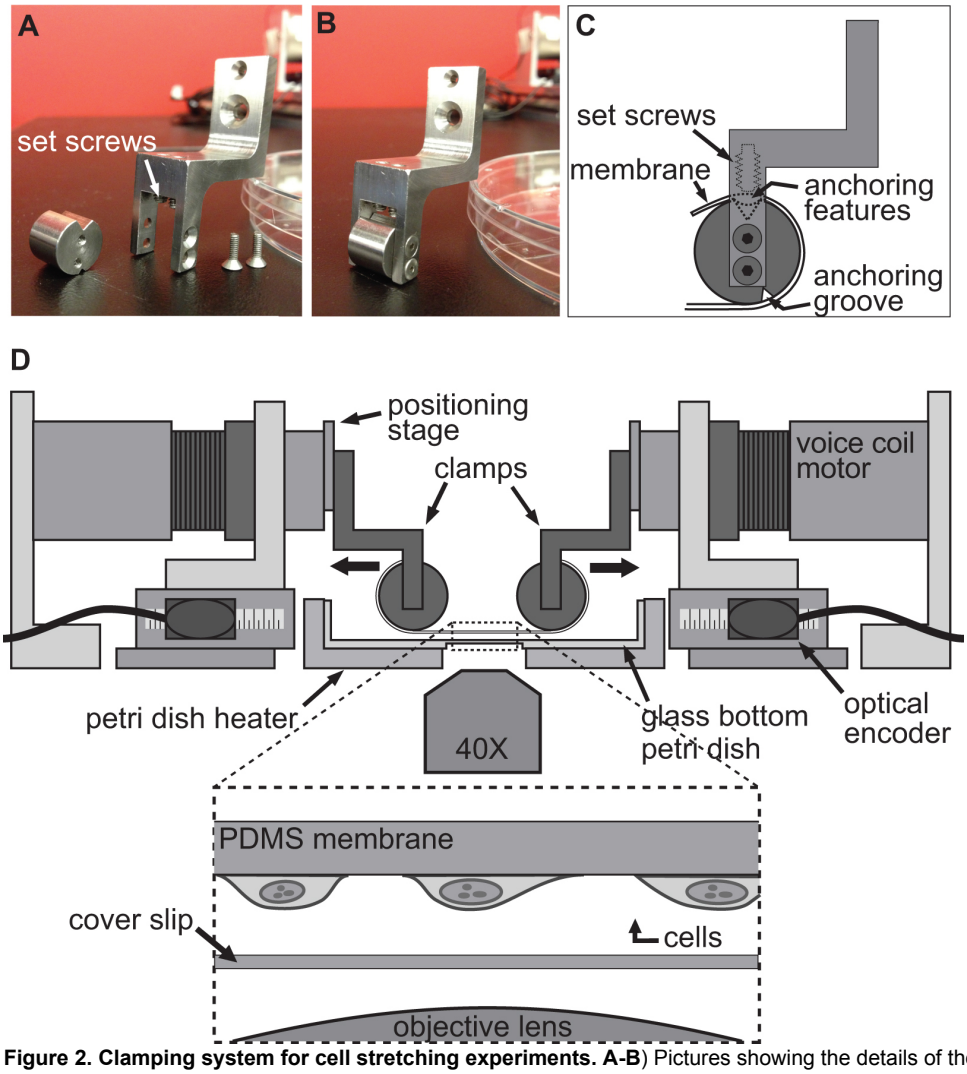

Figure 2. Clamping system for cell stretching experiments. A-B) Pictures showing the details of the clamps used to attach the PDMS substrate to the voice coil motors for stretching. **C**) The substrate is wrapped around the cylindrical part of the clamp with its anchoring features sitting into the groove at the top. Then the substrate is secured using the setscrews that push the substrate/anchoring features into the top groove. **D**) Illustration of the BAXS platform with the clamps holding the substrate in place. The inset shows a detailed view of the substrate with cells attached to it sitting just above a cover slip and the microscope objective.

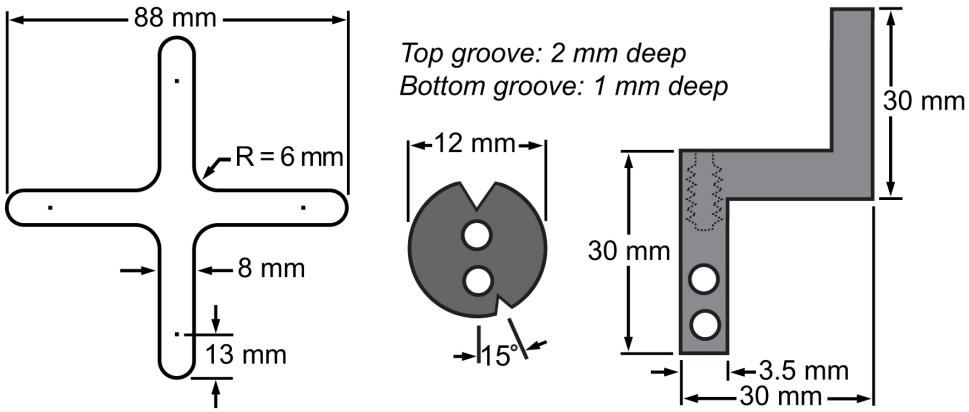

Figure 3. Bill of materials of the membrane and its clamping system. Drawings showing the dimensions of the principal parts integrated to the biaxial platform to perform cell stretching experiments.

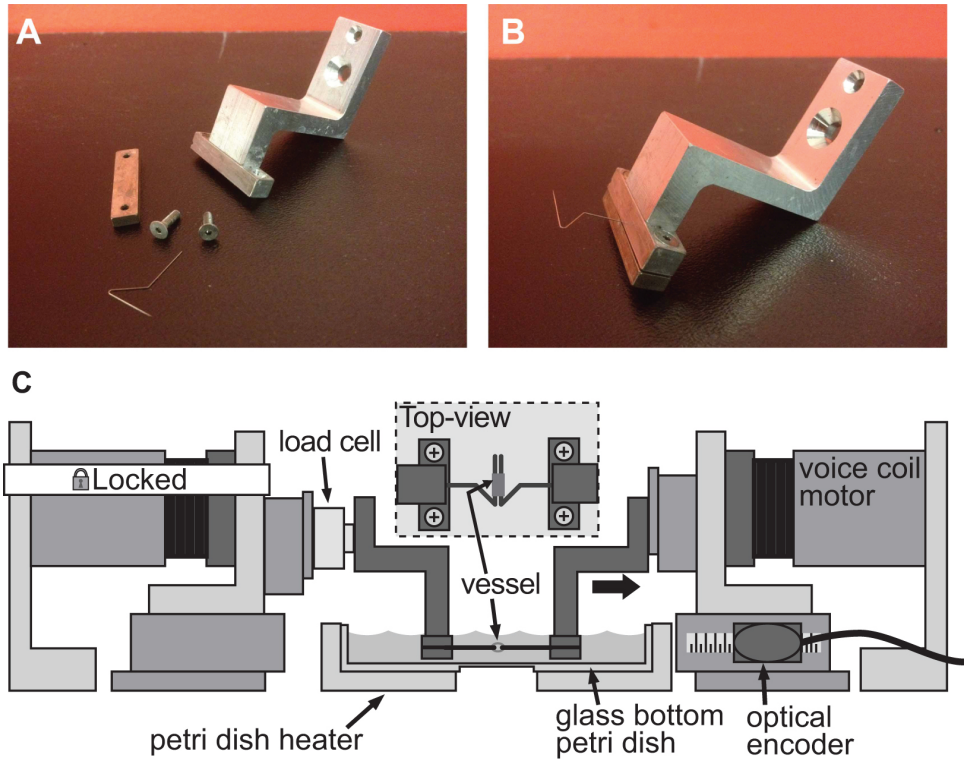

Figure 4. Example of a clamping system for stiffness assessment of small caliber vessels. A-B) Detailed pictures of the clamping system used to induce deformation in a 1 mm diameter mouse aorta. Stainless steel pins were carefully shaped into open triangles to allow the vessel to slide on both pins. **C**) Illustration of the BAXS platform with the clamps holding the vessel and a load cell attached between the fixed motor and the left clamp. The inset shows a detailed top-view of the vessel mounted on the pins.

Protocol

1. Mechanical Deformation of Single Cells

1. Fabrication of a PDMS Substrate with Embedded Fluorescent Beads
   Prior to fabrication of the substrate, fluorescent microspheres in water solution are resuspended in isopropanol to enhance bead mixing in the PDMS due to its hydrophobic nature.
   1. Pipette 500 µl of fluorescent microspheres into a 1.5 ml microcentrifuge tube and centrifuge at 16,200 x g for 10 min.
   2. Discard the supernatant and add 500 µl of isopropanol followed with 5 min of vortexing. Put the vial aside overnight in the dark in order to allow any large particles aggregates to sediment.
   3. The next morning, carefully remove the supernatant to a clean microcentrifuge vial. This bead solution can be used to fabricate more than 5 substrates. NOTE: The bead solution will continue to sediment for the next 3 days. Be careful to avoid resuspending the pellet.
   4. Pour 0.5 g of the curing agent provided with the PDMS kit in a 1.5 ml microcentrifuge vial using a scientific balance. By successive steps, add a total of 90 µl of beads (in six 15 µl additions), vortexing for 1 min between each addition. Set aside.
   5. Weigh 10 g of PDMS and mix for at least 12 min with the 0.5 g of the curing agent supplemented with fluorescent beads.
   6. Fabricate an SU-8 2050 cross-shaped mold using standard photolithography techniques following manufacturer's instructions. The mold used has a height of 320 µm and an area of 13.4 cm^2 (**Figure 3**). The mold can contain 428 µl or 440 mg of PDMS.
   7. Pour 400 mg of the PDMS with beads in the cross-shaped mold using a transfer pipette and cure for 2 hr at 80 °C. After curing, peel off the substrate from the mold (**Figure 5A**). The substrate can be kept in a Petri dish at room temperature for 2 weeks without showing significant changes in its mechanical properties.
   8. Pour droplets of PDMS (curing agent:PDMS with a ratio of 1:20) in a Petri dish with a final size of approximately 4 mm in diameter and cure them upside down for 2 hr at 80 °C (**Figure 5B**). These anchoring features can be kept in a Petri dish for weeks. NOTE: Maintain the dish upside down to prevent the drops from flattening during the curing process.
   9. Air-plasma treat (30 sec at 30 W) the substrate and 8 anchoring features. Bind the features on each end of the substrate at a distance of 4 mm from the square shaped indent present on the substrate (**Figure 5C**).

2. Mounting Membrane on the Clamps
   1. Wrap each end of the substrate around the grooved cylindrical part of the clamps and secure it in place with the 2 setscrews from the top (**Figure 2B** and **Figures 5D-E**).
   2. Screw the 4 clamps on the clamp holder and pour PDMS (ratio 1:20) using a disposable transfer pipette at the interface between the substrate and the grooved cylindrical part of the clamps. Spread the uncured PDMS around the grooved cylindrical part using a 1.5 mm hex key.

3. Pour PDMS (1:20) in the grooves until completely filled by capillary action and cure the assembly at 80 °C for 2 hr (**Figure 5F**).

3. Seeding Cells on the Membrane
    1. Air-plasma treat (30 sec at 30 W) the whole assembly to sterilize and functionalize the substrate to allow for collagen coating.
    2. Functionalize the area of the substrate where cells will be seeded with 1 ml of 0.02 M acetic acid supplemented with 16 µg/ml of rat-tail collagen at room temperature for 1 hr. The desired final collagen density is 5 µg/cm^2.
    3. Rinse the substrate 3x with phosphate buffer and let it dry at room temperature for at least for 10 min.
    4. Add 40 µl of culture medium supplemented with 10% fetal bovine serum and 1% penicillin-streptomycin containing 2,000 cells in the center portion of the substrate to cover an area of 1 cm^2 (cell density: 20 cells/mm^2). Cell density can be altered according to experimental requirements.
    5. Put the whole assembly in a standard cell culture incubator with the substrate facing up with the drop of culture medium containing cells on it. NOTE: The assembly must be kept with the substrate facing up for at least 3 hr to allow cells to firmly attach it. To prevent evaporation, 30 µl of warm culture medium is added into the drop on the substrate every 45 min for 3 hr.
    6. After 3 hr, flip the whole assembly into a Petri dish filled with fresh culture medium to submerge the substrate and incubate overnight to allow cells to proliferate.
    7. The next day, prepare HEPES-buffered salt solution (HBSS; 20 mM of Hepes, 120 mM of NaCl, 5.3 mM of KCl, 0.8 mM of $MgSO_4$, 1.8 mM of $CaCl_2$, and 11.1 mM of dextrose). Adjust the pH to 7.4. NOTE: The HBSS solution has to be prepared daily and kept at 37 °C during the experiments. This physiological solution is used to maintain the cells on the microscope stage by mimicking the normal tissue/blood environment.
    8. Mount the set-up on inverted phase contrast or fluorescent microscope Mount the clamp-substrate assembly on the BAXS platform and motors. Fill the Petri dish inside the Petri dish heater with HEPES buffer (**Figure 2D**).

2. Stiffness Measurement of Small Caliber Vessels

1. Preparation
    1. Krebs physiological solution: Prepare a solution of 118.1 mM NaCl, 11.1 mM D-glucose, 25 mM $NaHCO_3$, 4.7 mM KCl, 1.2 mM $MgSO_4$, 1.2 mM KH_2PO_4, and 2.5 mM $CaCl_2$. Adjust the pH to 7.4 and oxygenate the solution with carbogen medical gas (95% O_2/5% CO_2) for 30 min. NOTE: The Krebs solution has to be prepared daily and kept at 37 °C during the experiments. This physiological solution is used to maintain the tissues alive by mimicking the normal tissue/blood environment.
    2. Gather instrumentation for the dissection and mechanical assessment of aortic vessels: surgical scissors, bended tweezers, micro-scissors, surgical dissecting microscope, 50 ml polypropylene centrifuge tubes, and 10 ml serological pipettes. The surgical and experiment procedure do not require any sterile conditions. Mount the clamps of the BAXS platform along with the load cell beforehand.

2. Tissue Isolation and Dissection
   All experimental procedures involving laboratory animals have to be approved by the Animal Care and Use Committee of the users' institution, which complies with the Health Guide for the Care and Use of Laboratory Animals of the users' country.
    1. Perform mouse euthanasia with the inhalation of 99% CO_2 (7 psi) in a Plexiglas chamber (**Figure 6A**).
    2. Open mouse abdomen and cut the thoracic aorta to bleed the mouse.
    3. Remove the diaphragm, the thoracic cage and the lung lobes (**Figure 6B**). NOTE: To minimize the risk of damaging the tissue, keep the heart attached to the aorta and avoid touching the vessel directly but manipulate it using the heart.
    4. Remove the heart, the aortic root and the thoracic aorta by gently cutting between the vessel and the spine. NOTE: Do not induce any elongation in the vessel during the excision to keep the inner structure of the tissue intact (**Figure 6C**).
    5. Immediately immerse and keep the heart and aorta in Krebs solution.
    6. Cut and carefully wash the aorta in Krebs solution to remove any blood clots. Remove connective tissue using micro-scissors, tweezers and surgical dissecting microscope (**Figure 6D-E**). NOTE: Keep all the vessel length and use the aortic root to determine the vessel orientation.

3. Vessel Dimension Determination and Mounting
   To determine the stiffness of the vessel, the unloaded vessel dimensions are required and can be determined with a calibrated microscope.
    1. Cut an aortic ring of about 2 mm in length and precisely measure its length using a calibrated microscope setting (**Figures 6F-G**). Put this segment aside in Krebs solution.
    2. Cut another aortic ring as small as possible between each of the 2 mm segments (**Figure 6F**). Put this small segment on a microscope glass slide with the lumen facing up and measure the wall thickness using a calibrated microscope setting (**Figure 6H**).
    3. Fill the Petri dish on the BAXS platform with Krebs solution and insert the 2 mm aorta ring segment on the pulling pins (inset in **Figure 4C**).

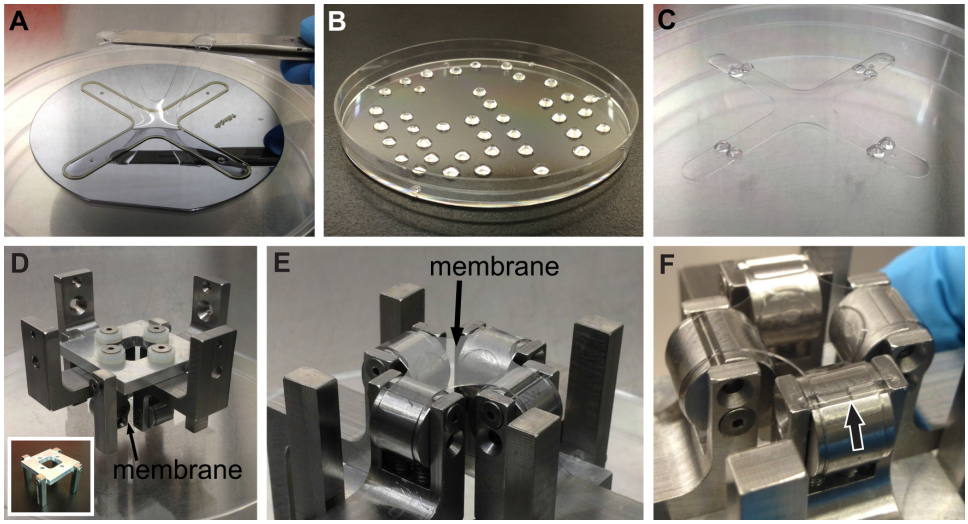

Figure 5. PDMS substrate fabrication and mounting. A) After curing, the substrate is carefully peeled off the SU-8 2050 mold and put aside in a Petri dish. **B**) Anchoring features made out of PDMS and help to secure the substrate on the clamps. **C**) Substrate with anchoring features ready for mounting. **D**) The substrate is mounted on the 4 clamps, which are then mounted on the clamp holder (see inset). **E**) Detailed picture of the substrate mounted on the 4 clamps. **F**) Procedure of pouring PDMS in the groove underneath the substrate. The arrow shows the PDMS slowly filling the groove by capillarity.

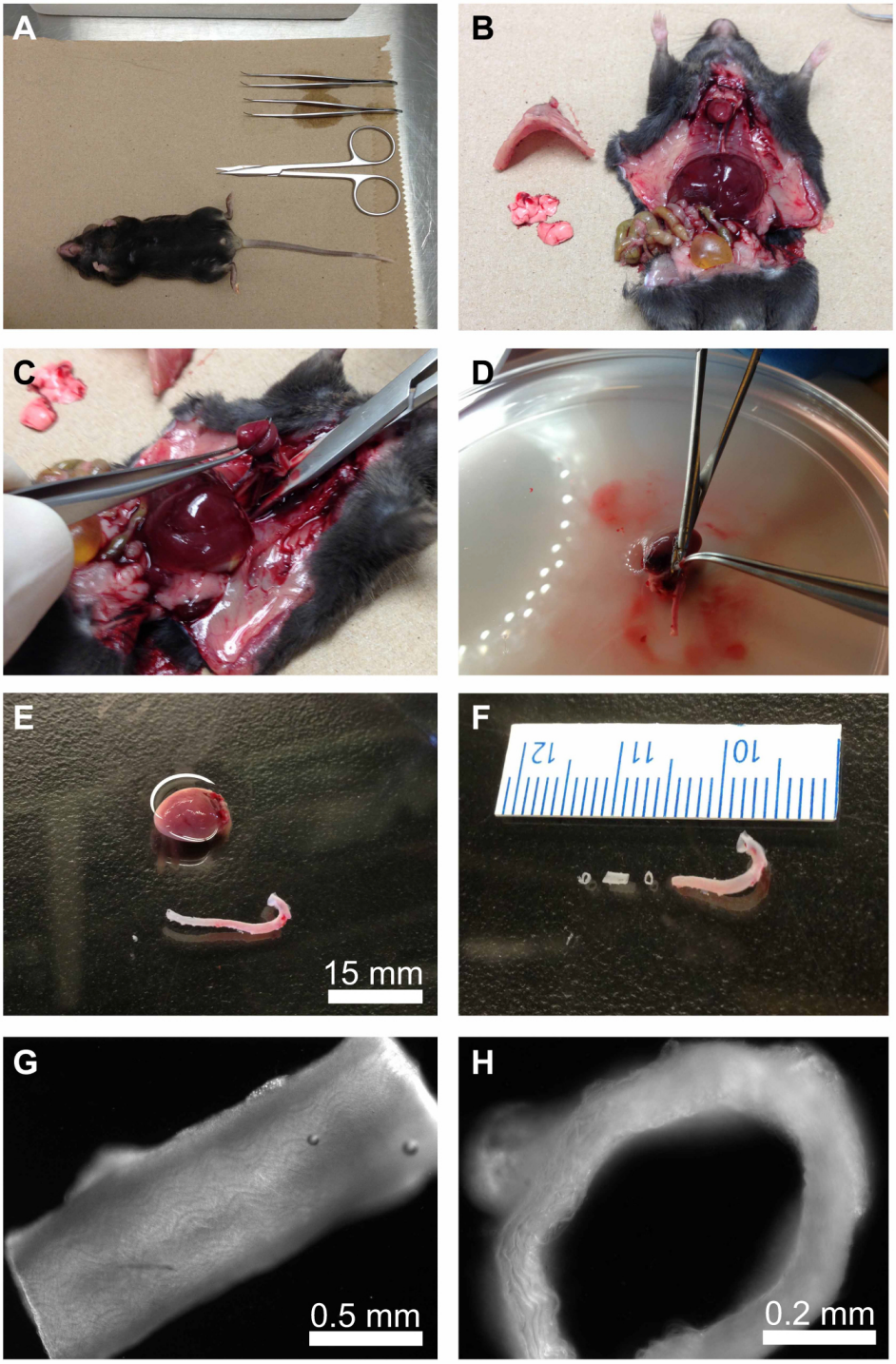

Figure 6. Preparation and isolation of the thoracic aorta. A) Preparing surgical instruments and the euthanized mouse. **B**) Through a longitudinal abdominal incision, the thoracic cage and lung lobs are removed. **C**) The aorta is carefully removed using the heart to manipulate the tissue. **D**) The heart and aorta are put in Krebs physiological solution. The aorta is cleaned by removing all connective tissues. **E**) Detailed picture showing the heart and aorta. **F**) Aorta segment used for stiffness assessment along with small segments used for thickness measurement. **G-H**) The precise length (**G**) and thickness (**H**) of each vessel segments are evaluated using an inverse microscope and an analysis program.

Representative Results

Cell Stretching

The BAXS platform was used to investigate the mechanical response of the nucleus in single mouse myoblast cells (C2C12) exposed to a substrate deformation of 25%. Myoblast cells are found in muscle tissue and are constantly exposed to mechanical stretch and compression *in vivo*. The shape and mechanical properties of the cell nucleus have shown to play a major role in the regulation of gene expression and transcriptional activity[20,21] and also in a variety of developmental defects and diseases such as Hutchinson-Gilford progeria syndrome (HGPS), Emery-Dreifuss muscular dystrophy (EDMD), dilated cardiomyopathy, premature aging and cancer[22-25]. Therefore, understanding how forces from the external mechanical microenvironment affect the structure and function of the nucleus is of extreme interest. The BAXS platform was used to investigate the transmission of force from the microenvironment to the nucleus by stretching the substrate parallel to its major or minor axis. **Figures 7A-F** illustrates the capabilities of the platform for inducing a deformation in the substrate along two orthogonal directions. Moreover, the BAXS platform can induce complex strain fields in the substrate in addition to standard uniaxial of equi-biaxial strain fields. **Figures 7G-H** illustrates the flexibility provided by independent control of the strain field along two orthogonal directions, allowing us to either produce a standard (compressive) or pure (non-compressive) uniaxial strain field. The BAXS platform is able to produce a pure uniaxial strain field by slightly pulling the substrate in the direction perpendicular to the principal stretching direction (**Figure 7G**) to compensate for the compression present in the substrate along this direction during a standard uniaxial stretch (**Figure 7H**).

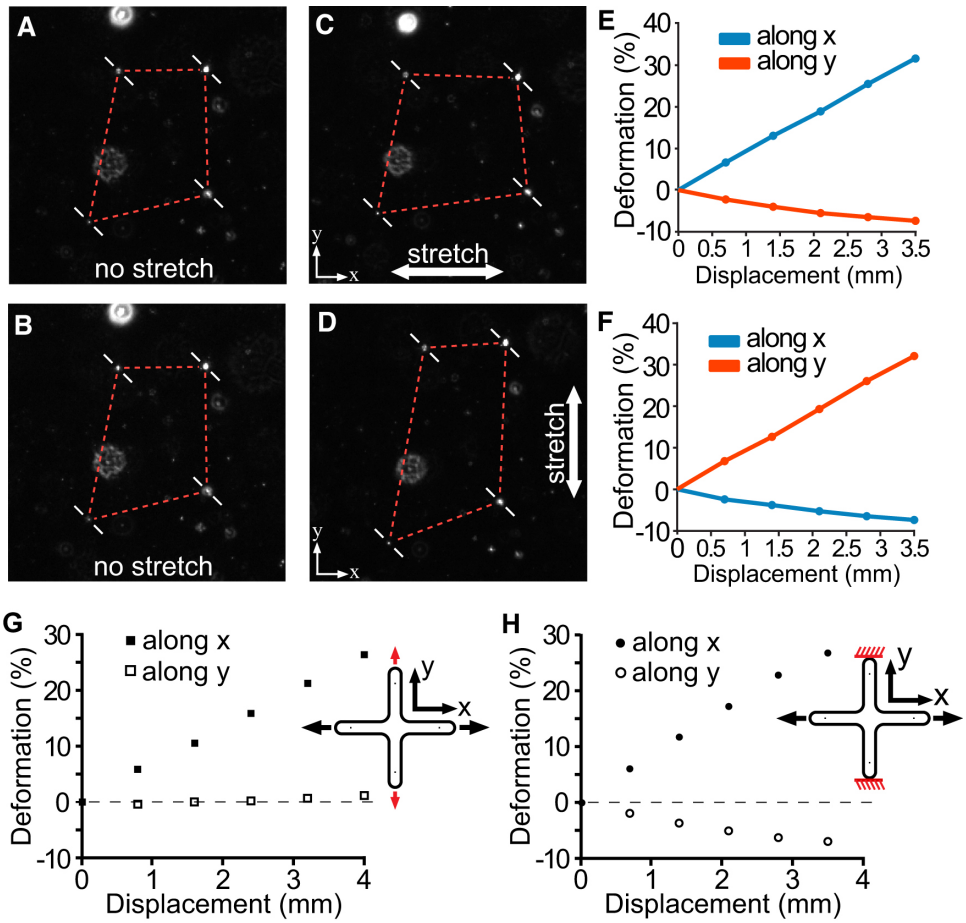

Figure 7. Displacement-deformation relationships from performing standard and pure uniaxial stretching. A-B) Fluorescent beads are manually selected on the first frame of the video and tracked from one frame to the other until maximum stretch is reached along the horizontal (**C**) and vertical (**D**) directions. A MATLAB script automatically computes the components of the Green strain tensor for each frame and produces a calibration curve of the strain in respect to motor displacements[27]. **E-F**) The blue and red lines correspond to the component of the Green strain tensor along the horizontal and vertical directions respectively. **G**) Stretching the same substrate by 4 mm along the x axis and slightly stretching along the y axis by 1.5 mm (highlighted in red) produces a pure uniaxial field with no compressive deformation in the substrate. H) Stretching the substrate along the x-axis by 3.5 mm produces a deformation of 25% and a compressive deformation of 7% when the ends of the substrate along the vertical axis are fixed (highlighted in red).

With the ability to perform live-cell microscopy imaging during stretch, nuclei were stained with a live-cell fluorescent dye, which binds to DNA (Hoescht 33342). In general, C2C12 cells possess elliptical nuclei with a major and minor axis. First, cells were identified in which the major or minor nuclear axes were oriented parallel to the horizontal stretching direction. At this point, cells were stretched by 25% along each orthogonal stretching axis while acquiring images of the undeformed and deformed nucleus between each stretching cycles (**Figures 8A-I**). In this manner we could assess the deformability of the nucleus along its major and minor axis under a precisely controlled substrate deformation. Ovuscule, an ImageJ plugin, was used to determine the length of the major and minor nuclear axes. These lengths were recorded during the undeformed state and when the nucleus was sequentially stretched along its major and minor axes (**Figures 8G-I**). To calculate the deformation of the nucleus along its minor and major axes, the relative change in length along each axis in the stretched and undeformed states was computed:

$$\varepsilon = \frac{L_1 - L_0}{L_0}$$

where ε is the deformation, L_1 is the deformed length and L_0 is the undeformed length.

The deformability of the nucleus in C2C12 exhibits a mechanical anisotropy as it displays a significantly higher deformability along its minor axis (6.3±1.1%) in comparison to its major axis (3.0±0.6%) (**Figure 8J**). In addition, we also examined the role of the actin and microtubule cytoskeleton in regulating nuclear deformability. This was achieved by depolymerizing the actin filaments or microtubules selectively using cytochalasin-D and nocodazole, respectively. Depolymerizing the actin filaments or the microtubules was found to induce a loss of the anisotropic deformability of the nucleus (**Figure 8J**). These results support the findings that cytoskeletal components transmit forces to the nucleus from the substrate and are also essential for preserving the natural mechanical behavior of the nucleus during deformation[25].

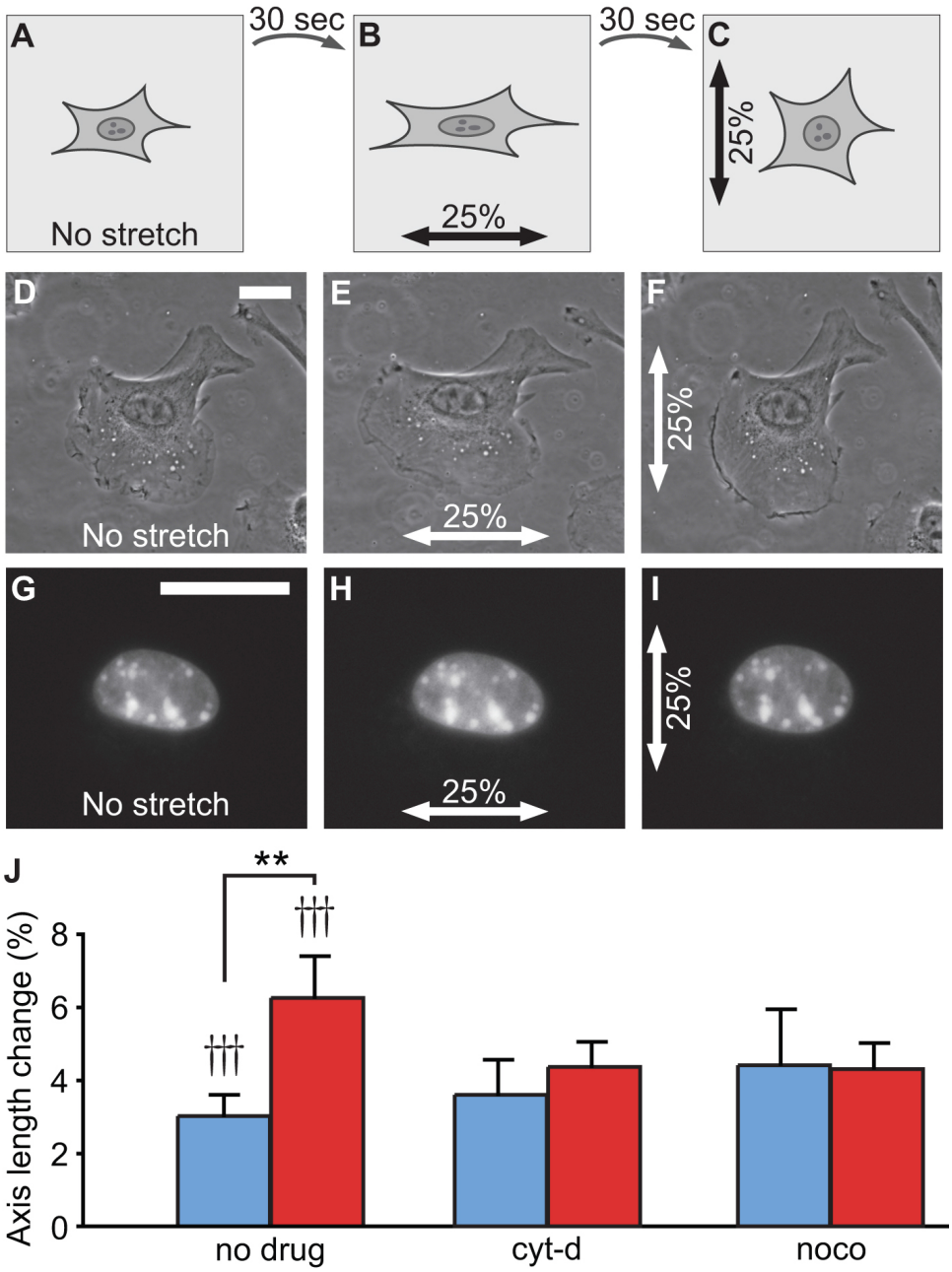

Figure 8. Stretching protocol and nuclear deformability. A-C) Schematic illustration of the stretching protocol of a single cell with its nucleus oriented horizontally. Phase contrast images (**D-F**) and epi-fluorescent images (**G-I**) of a cell stained with DNA-specific fluorescent dye. This image sequence illustrates a typical cell stretching experiment where the same cell is exposed to orthogonal deformation fields. Scale bars are 25 µm. **J**) C2C12 shows anisotropic nuclear deformability with the minor axis deforming significantly more than the major axis. In actin- or microtubule-deprived cells (cyt-d and nocodazole, respectively), this anisotropy disappears. In all conditions, nucleus deformations are significantly different from zero under a substrate deformation of 25%. ** *p*-value < 0.01, paired t-test. †† *p*-value < 0.01, ††† *p*-value < 0.001, one-sample t-test.

Vessel Stiffness Assessment

Recently, our group investigated the effect of the chronic over-expression of Heat Shock Protein-27 ($HSP27^{o/e}$) on the formation of aortic plaques in an atherosclerosis-prone mouse model ($apoE^{-/-}$)[26]. We showed that HSP27 acts as an atheroprotective protein that reduces plaque lipid and macrophage abundance and increases the intimal smooth muscle cells and collagen content (**Figures 9A-B**). To determine the impact of this histological remodeling on vessel mechanical properties, the BAXS platform was used to measure aortic stiffness.

Figure 9C shows a typical stress-strain curve from the tensile stretching of an aortic ring. To quantify stiffness, the incremental modulus was computed from stress-strain curves at a deformation of 30%. The stiffness is the slope of the tangent to the curve. By introducing a load cell onto one of the BAXS platform motors, the simultaneous acquisition of displacement and force data is possible. The displacement-force curves

were converted into stress-strain curves based on the undeformed dimensions of each aortic ring. The stress and strain are computed using the following formulas:

$$\varepsilon = \frac{L_1 - L_0}{L_0}$$

$$\sigma = \frac{F}{A_0}$$

where ε is the deformation, L_1 is the deformed length, L_0 is the undeformed length, s is the stress, F is the force and A_0 is the undeformed area of the tissue under loading. In the specific case of an aortic ring, the undeformed area (A_0) is twice the thickness of the ring times the length of the segment.

Each sample was deformed cyclically with a maximum deformation of 40% at a displacement rate of 50 µm/sec for 12 cycles with the first 11 cycles allowing preconditioning of the tissue and the last one for data acquisition. We found that the stiffness of aortic segments of apoE$^{-/-}$HSP27$^{o/e}$ mice (62.8±3.0 kPa) were significantly increased by 41% compared to the apoE$^{-/-}$ control mouse model (44.4±3.8 kPa) (**Figure 9D**).

Taken together, the mechanical assessment combined with the vessel and plaque histology demonstrated that the over-expression of HSP27 is characterized by increased vessel stiffness and collagen/smooth muscle cell content. These results suggest that HSP27 could potentially increase stability of atherosclerotic lesions and therefore decrease the risk of plaque rupture.

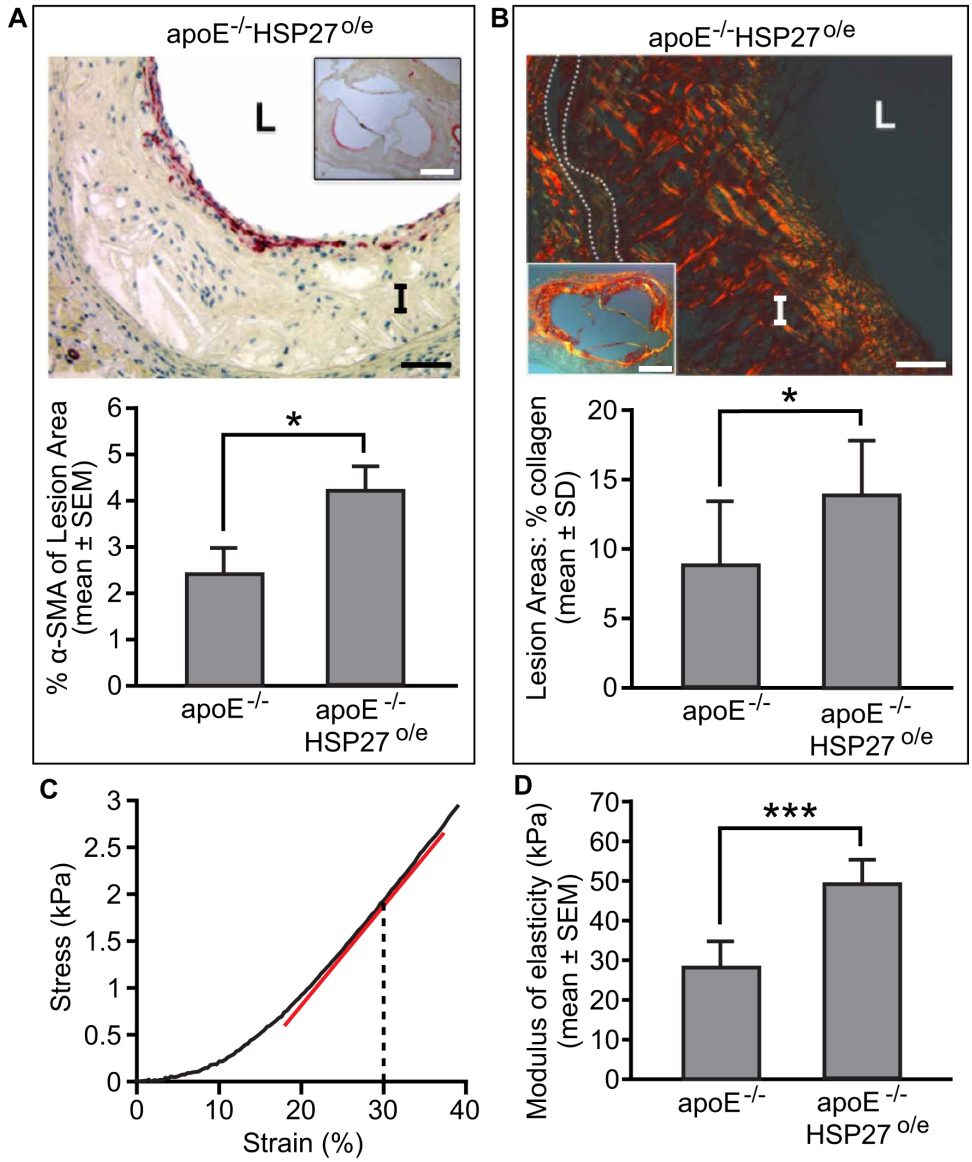

Figure 9. Effect of HSP27 over-expression on vessel stiffness. We showed that HSP27 modified the histological composition of atherosclerosis lesions by increasing intimal smooth muscle cells (**A**: anti-α-SMA) and collagen content (**B**: picrosirius red stain). **C**) Typical stress-strain curve obtained from stretching an aortic vessel where the stiffness is computed at 30% of strain. The stiffness is the slope of the tangent (red line) to the curve. **D**) Chronic over-expression of HSP27 increases vessels rigidity in comparison of control apoE$^{-/-}$ mice model (**D**). Scale bars in (**A**) and (**B**) are both 40 µm and 400 µm in the insets. L=lumen, I=intima, dotted lines delineates the media. * *p*-value < 0.05, one-way ANOVA. *** *p*-value < 0.001, one-way ANOVA. Figure adapted from the work of Cuerrier *et al*[26].

Discussion

The BAXS platform presented here facilitates numerous experiments in the study of mechanobiology, from investigations of single cells to whole tissues. In addition, the platform is highly flexible and configurable, allowing for numerous mechanical stimulation experiments and multi-axial tensile testing. The platform also enables the maintenance of cells and tissues in physiological conditions and allows for simultaneous microscopy during stretching experiments. The two experiments described in the previous sections demonstrate the versatility of the BAXS platform when using a proper set of mounting clamps. A modular and customizable sample mounting system, optical access and the possibility to add additional sensors (for example a load cell), open up numerous possibilities for additional types of experiments to be performed.

The protocol presented above contains many critical steps that must be performed adequately in order to produce the best results. Within the cell stretching protocol, mounting the PDMS substrate on to the clamps demands delicate and precise manipulation. The PDMS substrate must be well centered with respect to the four clamps to avoid unwanted lateral movements of the substrate during stretching. Such lateral movements can make the tracking of the cells difficult during stretching experiments. Also, it is critical to monitor the evaporation of the drop of culture medium during cell seeding when the substrate is facing up in the incubator. Depending on how often the incubator door is opened during the process, the evaporation rate can change. Within the vessel stretching protocol, the most critical step is the measurement of the dimensions of the sample to be tested. These dimensions must be as accurate as possible as they are involved in the calculation of the tissue stiffness and

therefore have a direct impact on the results. Having the same person perform vessel dimension measurements will aid in reducing variability between samples.

The fabrication of the clamps used to pull on the PDMS substrate during cell stretching experiments involved several development cycles. The first version of the clamps did not have an anchoring groove located at the bottom of the cylindrical parts (**Figure 2B**). Without this groove, the substrate slipped along the cylindrical part, inducing a significant variability in substrate deformation over time. With the presence of the groove and the addition of cured PDMS (**Figure 5F**), the substrate no longer slips. This experimental setup produces a constant deformation in the substrate over time. For tissue stretching experiments, choosing the proper load cell is also very important. The load cell used here has a low load range (up to 150 g), which is adequate for the samples tested here. The very sensitive load cell required for measuring pulling forces on small samples possessed a relatively low signal to noise (s/n) ratio. To improve the s/n ratio and therefore improve resolution, the load cell was electrically isolated from the voice coil motor and any metal parts using plastic screws and spacers. In this manner a high s/n ratio with a resolution of 0.03 g was obtained. For softer samples, the use of a lower range load cell is recommended in order to maintain high resolution.

Currently, the major limitation of the BAXS platform is the ability to perform long term stretching experiments due to the evaporation of the HBSS buffer over time. Water evaporation increases solute concentration that can potentially have an effect on cells. With the current configuration of the BAXS platform, it is difficult to have an experiment that would mechanically stimulate cells or tissues over days as the buffer in which the cells and tissues are submerged has to be supplemented with liquid over time. In the current setting, the evaporation rate is about 0.9 ml/hr from an initial volume of 25 ml of HBSS buffer solution. The current setting is ideal for short-term experiments. To perform reliable cell and tissue stretching experiments over longer periods of time, two additions are suggested: 1) A fluidic system for maintaining buffer volume, and 2) the addition of a commercial or home built incubator chamber enclosing the whole system in order to maintain constant humidity and temperature and provide a 5%/95% CO_2/air atmosphere. Regarding the option of stretching vascular tissues, the setup described above allowed us to measure the stiffness of small caliber vessels. It is important to use pins with a proper diameter to make sure that they will not deform during stretching, but are small enough to fit into the vessel lumen. Not taking this detail into account could introduce inaccuracy in the measured deformation of the tissue.

In-vivo, tissue-embedded cells are exposed to mechanical forces and strains that vary both spatially and temporally, but more importantly they are often multi-axial. A good example is the mechanical behavior of the vasculature walls in response to hemodynamic forces. The combination of local hemodynamic forces[28-30] with the anisotropic properties of vascular tissues[13,14,16,27] result in a complex mechanical microenvironment, which exposes endothelial and vascular smooth muscle cells to complex multi-axial and cyclic strain fields. Although existing cell stretching experiments have greatly contributed to the basic understanding of mechanotransduction and mechanobiology, they have traditionally relied on idealized uniaxial or equi-biaxial strain fields that do not reproduce complex *in vivo* strain fields[8-10,19,29,31-34]. The BAXS platform allows anisotropic biaxial cell stretching with simultaneous live-cell microscopy. The ability to control the deformation of the substrate along two orthogonal directions allows us to have full control over the strain field. This enables the production of complex strain fields in addition to simple uniaxial and equi-biaxial strain fields. Moreover, the platform allows us to dynamically change the direction of the strain field within the same stretching experiment.

The option of integrating a modular and custom clamping system opens up the possibility for many applications in cell mechanobiology and tissue mechanics using a single stretching platform. For example, with proper clamping systems[13,27], this platform can perform planar uniaxial and biaxial tensile testing of biological tissues. In this manner, the mechanical properties of any tissue, cut in a rectangular or square shape, can be quantified along two orthogonal axes in a single experiment. In addition, performing histological analyses after mechanical stimulation can reveal stretch-induced structural changes in tissues. Torsion is also a very important type of mechanical loading for muscle tissues and ligaments[35]. This platform provides the potential to design a clamping system that could induce a rotation around the stretching axis to produce a combinatory mechanical loading involving torsion and tension. It is also possible to assess larger caliber vessels with appropriate mounting pins. Studying cellular responses following mechanical deformation is also under intense investigation. The BAXS platform offers a unique feature of changing the direction and the complexity of strain field within the same experiment in addition to allowing for simultaneous imaging. Importantly, multi-modal forms of microscopy are still possible, as the platform does not interfere with the optical axis of the microscope. This is an important feature as the structural and biochemical live-cell responses to mechanical deformation can be measured. Taken together, the BAXS platform design possesses several important features that facilitate its use for single cell and whole tissue experiments. By employing a modular clamping system and the addition of up to four possible load cells, the BAXS platform can be employed for a multitude of experiments. This article shows details of two examples of experiments; however the modularity and flexibility of the system can be further exploited to investigate many diverse aspects of mechanobiology at the sub-cellular, cellular and whole tissue length scales.

Disclosures

The authors declare that they have no competing financial interests.

Acknowledgements

DT was supported by a postdoctoral studentship from le Fonds de Recherche du Québec-Nature et Technologies (FQRNT) and a MITACS Elevate Strategic Fellowship. CMC was supported by a postdoctoral studentship from le Fonds de Recherche en Santé du Québec (FRSQ) and the Ernest and Margaret Ford cardiology endowed research fellowship from the University of Ottawa Heart Institute. EOB was supported by operating grants MOP80204 from the Canadian Institute for Health Research (CIHR) and T6335 from the Heart and Stroke Foundation of Ontario. The CIHR and Medtronic collectively provide EOB with a peer-reviewed Research Chair (URC #57093). AEP is funded by the Natural Sciences and Engineering Research Council (NSERC) Discovery Grant, an NSERC Discovery Accelerator Supplement and gratefully acknowledges the support of the Canada Research Chairs (CRC) program and an Early Researcher Award from the Province of Ontario.

References

1. Yim, E.K. and Sheetz, M.P. Force-dependent cell signaling in stem cell differentiation. *Stem Cell Res Ther.* **3**, 41 (2012).
2. Vogel, V. and Sheetz, M. Local force and geometry sensing regulate cell functions. *Nat Rev Mol Cell Biol.* **7**, 265–275 (2006).
3. Wang, N., Tytell, J.D., and Ingber, D.E. Mechanotransduction at a distance: mechanically coupling the extracellular matrix with the nucleus. *Nat Rev Mol Cell Biol.* **10**, 75–82 (2009).
4. Ingber, D.E. Mechanobiology and diseases of mechanotransduction. *Ann Med.* **35**, 564–577 (2003).
5. Janmey, P.A. and Miller, R.T. Mechanisms of mechanical signaling in development and disease. *J Cell Sci.* **124**, 9–18 (2011).
6. Bukoreshtliev, N.V., Haase, K., and Pelling, A.E. Mechanical cues in cellular signalling and communication. *Cell Tissue Res.* **352**, 77–94 (2013).
7. Chen, Y., Pasapera, A.M., Koretsky, A.P., and Waterman, C.M. Orientation-specific responses to sustained uniaxial stretching in focal adhesion growth and turnover. *Proc Natl Acad Sci USA.* **110**, E2352–E2361 (2013).
8. Rosenzweig, D.H., Matmati, M., Khayat, G., Chaudhry, S., Hinz, B., and Quinn, T.M. Culture of Primary Bovine Chondrocytes on a Continuously Expanding Surface Inhibits Dedifferentiation. *Tissue Eng Part A.* **18**, 2466–2476 (2012).
9. Balachandran, K. *et al.* Cyclic strain induces dual-mode endothelial-mesenchymal transformation of the cardiac valve. *Proc Natl Acad Sci USA.* **108**, 19943–19948 (2011).
10. Steward, R., Cheng, C.M., Ye, J., Bellin, R., and LeDuc, P. Mechanical stretch and shear flow induced reorganization and recruitment of fibronectin in fibroblasts. *Sci Rep.* **1**, (2011).
11. Wang, D., Xie, Y., Yuan, B., Xu, J., Gong, P., and Jiang, X. A stretching device for imaging real-time molecular dynamics of live cells adhering to elastic membranes on inverted microscopes during the entire process of the stretch. *Integr Biol (Camb).* **2**, 288–293 (2010).
12. Haskett, D., Johnson, G., Zhou, A., Utzinger, U., and Vande Geest, J. Microstructural and biomechanical alterations of the human aorta as a function of age and location. *Biomech Model Mechanobiol.* **9**, 725–736 (2010).
13. Duprey, A., Khanafer, K., Schlicht, M., Avril, S., Williams, D., and Berguer, R. *In vitro* characterisation of physiological and maximum elastic modulus of ascending thoracic aortic aneurysms using uniaxial tensile testing. *Eur J Vasc Endovasc Surg,.* **39**, 700–707 (2010).
14. Tremblay, D. *et al.* A comparison of mechanical properties of materials used in aortic arch reconstruction. *Ann Thorac Surg.* **88**, 1484–1491 (2009).
15. Khanafer, K., Duprey, A., Zainal, M., Schlicht, M., Williams, D., and Berguer, R. Determination of the elastic modulus of ascending thoracic aortic aneurysm at different ranges of pressure using uniaxial tensile testing. *The Journal of thoracic and cardiovascular surgery.* **142**, 682-686 (2011).
16. Vande Geest, J.P., Sacks, M.S., and Vorp, D.A. The effects of aneurysm on the biaxial mechanical behavior of human abdominal aorta. *J Biomech.* **39**, 1324–1334 (2006).
17. Guolla, L., Bertrand, M., Haase, K., and Pelling, A.E. Force transduction and strain dynamics in actin stress fibres in response to nanonewton forces. *J Cell Sci.* **125**, 603–613 (2012).
18. Wang, J.H., Goldschmidt-Clermont, P., Wille, J., and Yin, F.C. Specificity of endothelial cell reorientation in response to cyclic mechanical stretching. *J Biomech.* **34**, 1563–1572 (2001).
19. Jungbauer, S., Gao, H., Spatz, J.P., and Kemkemer, R. Two characteristic regimes in frequency-dependent dynamic reorientation of fibroblasts on cyclically stretched substrates. *Biophys J.* **95**, 3470–3478 (2008).
20. Dahl, K.N., Ribeiro, A.J.S., and Lammerding, J. Nuclear shape, mechanics, and mechanotransduction. *Circ Res.* **102**, 1307–1318 (2008).
21. Shivashankar, G.V. Mechanosignaling to the cell nucleus and gene regulation. *Annu Rev Biophys.* **40**, 361–378 (2011).
22. Chiquet, M., Gelman, L., Lutz, R., and Maier, S. From mechanotransduction to extracellular matrix gene expression in fibroblasts. *Biochim Biophys Acta.* **1793**, 911–920 (2009).
23. Sullivan, T. *et al.* Loss of A-type lamin expression compromises nuclear envelope integrity leading to muscular dystrophy. *J Cell Biol.* **147**, 913–920 (1999).
24. Lammerding, J. *et al.* Lamin A/C deficiency causes defective nuclear mechanics and mechanotransduction. *J Clin Invest.* **113**, 370–378 (2004).
25. Tremblay, D., Andrzejewski, L., Leclerc, A., Pelling, A. E. Actin and microtubules play distinct roles in governing the anisotropic deformation of cell nuclei in response to substrate strain. *Cytoskeleton.* Accepted (2013).
26. Cuerrier, C.M. *et al.* Chronic over-expression of heat shock protein 27 attenuates atherogenesis and enhances plaque remodeling: a combined histological and mechanical assessment of aortic lesions. *PLoS ONE.* **8**, e55867 (2013).
27. Tremblay, D., Cartier, R., Mongrain, R., and Leask, R.L. Regional dependency of the vascular smooth muscle cell contribution to the mechanical properties of the pig ascending aortic tissue. *J Biomech.* **43**, 2448–2451 (2010).
28. Barker, A.J., Lanning, C., and Shandas, R. Quantification of hemodynamic wall shear stress in patients with bicuspid aortic valve using phase-contrast MRI. *Ann Biomed Eng.* **38**, 788–800 (2010).
29. Haga, J.H., Li, Y.S.J., and Chien, S. Molecular basis of the effects of mechanical stretch on vascular smooth muscle cells. *J Biomech.* **40**, 947–960 (2007).
30. Frydrychowicz, A. *et al.* Time-resolved magnetic resonance angiography and flow-sensitive 4-dimensional magnetic resonance imaging at 3 Tesla for blood flow and wall shear stress analysis. *The Journal of thoracic and cardiovascular surgery.* **136**, 400–407 (2008).
31. Boccafoschi, F., Mosca, C., Bosetti, M., and Cannas, M. The role of mechanical stretching in the activation and localization of adhesion proteins and related intracellular molecules. *J Cell Biochem.* **112**, 1403–1409 (2011).
32. Yang, G., Crawford, R.C., and Wang, J.H.C. Proliferation and collagen production of human patellar tendon fibroblasts in response to cyclic uniaxial stretching in serum-free conditions. *J Biomech.* **37**, 1543–1550 (2004).
33. Goldyn, A.M., Rioja, B.A., Spatz, J.P., Ballestrem, C., and Kemkemer, R. Force-induced cell polarisation is linked to RhoA-driven microtubule-independent focal-adhesion sliding. *J Cell Sci.* **122**, 3644–3651 (2009).
34. Heo, S.J. *et al.* Fiber stretch and reorientation modulates mesenchymal stem cell morphology and fibrous gene expression on oriented nanofibrous microenvironments. *Ann Biomed Eng.* **39**, 2780–2790 (2011).
35. Zdero, R. *et al.* Linear and torsional mechanical characteristics of intact and reconstructed scapholunate ligaments. *J Biomech Eng.* **131**, 041009 (2009).

